

# An Electrochemical Strategy to Measure the Thickness of Electroactive Microbial Biofilms

Diego Millo\*<sup>[a]</sup>

*Dedicated to Dr. Claudio Tavagnacco on the occasion of his 60<sup>th</sup> birthday*

The study of electroactive microbial biofilms often requires knowledge of the biofilm thickness. Unfortunately, this parameter is, nowadays, only accessible through expensive microscopic techniques. This work overcomes this limitation by presenting a new strategy, exploiting the use of chronoamperometry (CA) alone. A mixed-culture biofilm is exposed to an O<sub>2</sub>-saturated solution during anode respiration to suppress its catalytic activity. Assuming that inactivation of the electrocatalytic process is caused by O<sub>2</sub> diffusion through the biofilm, a simple relation allows the use of the time constant extracted from the

fitting of the curve of the CA trace during inactivation for the straightforward and quantitative determination of biofilm thickness. The biofilm thickness obtained with this method obeys the expected trend reported for biofilm growth and is in agreement with optical measurements. Contrary to the techniques usually employed to determine biofilm thickness, this new strategy is very rapid, nondisruptive, inexpensive, and may become a convenient alternative with respect to expensive and time-consuming microscopic techniques.

## 1. Introduction

Converting pollutants present in wastewater into electricity and valuable chemicals is one of the main challenges of the coming decades. Fortunately, a technological solution is already at hand. In fact, bioelectrochemical systems (BESs) exploit the unique ability of certain microorganisms to oxidize the metabolic substrates present in wastewater and deliver the liberated electrons to insoluble electron acceptors outside the cell in a process called anode respiration.<sup>[1]</sup> Unfortunately, BES-based technologies need to be scaled up and their performances need to improve significantly so as to play a role in the global production of sustainable energy. To do this, fundamental research unraveling the functioning of BESs is warranted. However, characterizing the many different properties of microbial cells attached to an electrode, forming a multilayered aggregation denoted as a microbial biofilm, is not always straightforward. This is the case of biofilm thickness. This parameter, which is crucial to understand the fundamentals of long-range electron transfer, the effect of biofilm aging, and the accumulation of metabolic products inside the biofilm, is not always reported in research papers. This is because few researchers have access to microscopic techniques and—most

importantly—even fewer possess the expertise to treat the sample and process the data correctly. For instance, in the case of scanning electron microscopy (SEM), the biofilm must be removed from solution, dehydrated with a series of chemical procedures, and sputtered with a metal.<sup>[2]</sup> Confocal fluorescence spectroscopy requires biofilm staining,<sup>[3]</sup> whereas confocal resonance Raman microscopy, which does not require any biofilm manipulation, needs a specialist for data interpretation.<sup>[4]</sup> Surprisingly, even though confocal techniques are affected by severe aberrations, which lead to a considerable underestimation of the biofilm thickness, these limitations are seldom taken into account in research papers on electroactive microbial biofilms.<sup>[5,6]</sup> Moreover, not all electrochemical setups allow for the facile removal of the electrode and its placement under a microscope. Along with these microscopy-based methodologies, electrochemical methods are also available. On the one hand, as the biofilm thickness is proportional to the charge density measured during biofilm growth, one can use the area below the chronoamperometric trace monitoring biofilm growth to estimate this parameter.<sup>[4]</sup> However, this approach requires calibrating the system with one of the microscopic methods mentioned above to obtain the proportionality factor linking the charge density to biofilm thickness. On the other hand, the use of microelectrodes piercing the biofilms to map its pH and the redox potential profiles remains a niche application in the field of BESs.<sup>[7]</sup> To overcome the above limitations, I propose a new strategy to measure the thickness of electroactive biofilms based on chronoamperometry (CA) alone. This electrochemical technique is used to promote and monitor biofilm growth and is, thus, possible in all laboratories studying electroactive microbial biofilms. Importantly, contrary to the charge density method, it does not re-

[a] Dr. D. Millo

Department of Physics and Astronomy, VU University Amsterdam  
De Boelelaan 1081, 1081 HV, Amsterdam (The Netherlands)  
E-mail: d.millo@vu.nl

Supporting Information for this article is available on the WWW under <http://dx.doi.org/10.1002/celc.201402425>.

© 2015 The Authors. Published by Wiley-VCH Verlag GmbH & Co. KGaA. This is an open access article under the terms of the Creative Commons Attribution Non-Commercial NoDerivs License, which permits use and distribution in any medium, provided the original work is properly cited, the use is non-commercial and no modifications or adaptations are made.

quire any calibration before use. The proposed strategy consists of exposing an anode-respiring biofilm to a chemical agent that suppresses its electrocatalytic activity. Fitting the CA trace obtained during chemically induced biofilm inactivation allows the extraction of the time constant, which is linked to biofilm thickness through a simple relation.

## 2. Results and Discussion

In this work, a mixed culture biofilm and  $O_2$  were chosen as the electroactive microbial biofilm and the inactivating agent, respectively. Biofilm growth was monitored with CA and cyclic voltammetry (CV) (see the Supporting Information), revealing an electrochemical behavior consistent with mixed culture and *Geobacter sulfurreducens* biofilms.<sup>[8,9]</sup> The biofilm-coated electrode was then removed from the growth vessel and placed inside a gas-tight spectroelectrochemical cell operating in a three-electrode configuration and equipped with a flow system, allowing for rapid exchange of the working solution.<sup>[10]</sup> The electrode was kept at the constant potential of  $-0.085$  V versus a SCE under a flow of  $N_2$ -saturated buffer solution containing the metabolic substrate acetate. When current production reached a plateau, the working solution of the spectroelectrochemical cell was quickly replaced with  $O_2$ -saturated buffer solution.

As shown in Figure 1, bathing the biofilm with  $O_2$ -saturated buffer solution leads to a rapid loss of current production. It is worth noting that suppression of electrocatalytic activity for acetate oxidation is not attributed to biofilm removal, because electrocatalytic activity recovers completely after removing  $O_2$  from the cell compartment (see Figure S4). This important feature shows that this method is nondisruptive and several inac-

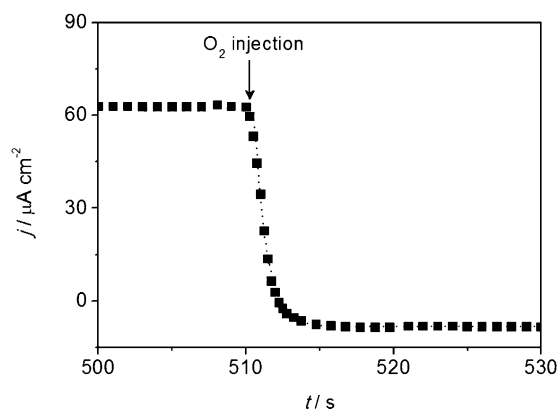


**Figure 1.** Representative CA trace of a mixed culture biofilm electrochemically grown on a smooth Ag electrode (biofilm growth was stopped at  $\sigma = 90$   $C\text{ cm}^{-2}$ ). Throughout the experiment, the biofilm was kept at a constant potential of  $-0.085$  V versus SCE. Before  $O_2$  injection ( $t < 510$  s), the electrode was subjected to a flow rate of  $0.01$   $\text{mL min}^{-1}$ . During  $O_2$  injection ( $t \approx 510$  s), the flow rate was kept at  $10$   $\text{mL min}^{-1}$  to allow fast and complete exchange of the working solution of the cell (internal volume of the cell is ca.  $50$   $\mu\text{L}$ ). The  $N_2$ - and the  $O_2$ -saturated working solutions had the following chemical composition:  $20$   $\text{mM}$  sodium phosphate buffer,  $6$   $\text{mM}$   $\text{NH}_4\text{Cl}$ ,  $4$   $\text{mM}$   $\text{KCl}$ , and  $10$   $\text{mM}$  sodium acetate ( $\text{pH } 7$ ). Black dots represent the CA data, whereas the dotted line is the monoexponential fitting to the experimental data. The coefficient of determination  $R^2$  is  $> 0.99$ .

tivation/recovery cycles may be performed on the same electrode sample. Importantly, biofilms were exposed to  $O_2$  for a limited span (ca. 2–5 min for each cycle), which was sufficient to suppress the electrocatalytic activity for acetate oxidation without producing toxic effects. Longer exposures to  $O_2$  may damage the biofilm irreversibly.<sup>[11]</sup> The CA trace fits to a monoexponential decay curve (Figure 1, dotted trace). This indicates that the rate-limiting step of biofilm inactivation is a one-step process. I, thus, hypothesized that this rate-limiting process is  $O_2$  diffusion through the biofilm. The expression correlating biofilm thickness with the time required for a noninteracting chemical agent to diffuse through the biofilm is shown in Equation (1):

$$L^2 = 0.97t_{90}D_e \quad (1)$$

where  $L$  [cm] is the biofilm thickness,  $t_{90}$  [s] is the time required for a solute added to the solution bathing a biofilm to attain 90% of the bulk fluid concentration at the base of a biofilm, and  $D_e$  [ $\text{cm}^2\text{s}^{-1}$ ] is the effective diffusion coefficient of the solute in the biofilm.<sup>[12,13]</sup> Equation (1) can be derived from the diffusion equation, as explained in the Supporting Information. Applying Equation (1) requires knowledge of the concentration of  $O_2$  at the biofilm–electrode interface, which is linked to the shape of the CA trace during inactivation. In fact, under the hypothesis that  $O_2$  diffusion is the rate-limiting step of biofilm inactivation, one can tentatively correlate the loss of current production in the CA profile of biofilm inactivation to the increase in  $O_2$  concentration inside the biofilm. Electrochemical detection of  $O_2$  inside the biofilm shows that  $O_2$  reaches the bottom of the biofilm in the time span predicted by Equation (1), and that its concentration at  $t > t_{90}$  is the same as in the bulk (see Supporting Information). Thus,  $t_{90}$  becomes the time required for  $O_2$  to diffuse through a flat biofilm and suppress 90% of its electrocatalytic activity for acetate oxidation.

$D_e$  is lower than the diffusion coefficient of the solute in water, owing to the presence of the biofilm. This reduction is described by the ratio  $D_e/D_{\text{aq}}$ , where  $D_{\text{aq}}$  is the diffusion coefficient of the solute in pure water. According to the literature, for light gases such as  $O_2$ ,  $D_e/D_{\text{aq}}$  is  $0.6$ .<sup>[12]</sup> Therefore, assuming  $D_{\text{aq}}[O_2]_{19^\circ\text{C}} = 17.1 \times 10^{-6}$   $\text{cm}^2\text{s}^{-1}$ ,  $D_e[O_2]_{19^\circ\text{C}}$  is  $10.3 \times 10^{-6}$   $\text{cm}^2\text{s}^{-1}$ .<sup>[14]</sup> A practical table reporting the values of  $D_{\text{aq}}$  at different temperatures is shown in the Supporting Information. Even though biofilms may not have an even thickness and uniform composition, this approach considers them as such. The validity of this approximation is supported by several studies and gives conservative estimates of biofilm thicknesses, as demonstrated in this work (see below).<sup>[12,13]</sup> Equation (1) describes the penetration of a noninteracting chemical agent. By noninteracting, it is meant that the chemical agent does not undergo reactions or sorption within the biofilm. Even though chemical reactions may occur in this case, their impact on the determination of biofilm thickness is likely to be negligible, as shown by the excellent correlation between biofilm thicknesses obtained with different methods (see below).

The best way to illustrate how to extract the biofilm thickness from the CA trace is by performing a calculation based on

the dataset shown in Figure 1. The monoexponential fitting of the experimental points (Figure 1, dotted line) gives a relaxation time constant  $\tau = 0.83$  s. By definition, this value is the time at which the electrocatalytic activity for acetate oxidation is reduced to 37%. To obtain the time at which 90% of the sample is inactivated, one must multiply  $\tau$  by 2.31 (see the Supporting Information). Accordingly,  $t_{90} = 2.31\tau = 1.92$  s. Introducing these data ( $t_{90} = 1.92$  s and  $D_e [\text{O}_2]_{19^\circ\text{C}} = 10.3 \times 10^{-6} \text{ cm}^2 \text{ s}^{-1}$ ) in Equation (1) gives  $L = 43.8 \mu\text{m}$ .

Figure 2 reports the biofilm thicknesses measured from the CA traces of biofilms whose growths were stopped at different charge densities  $\sigma$ . As expected, the biofilm thickness increases

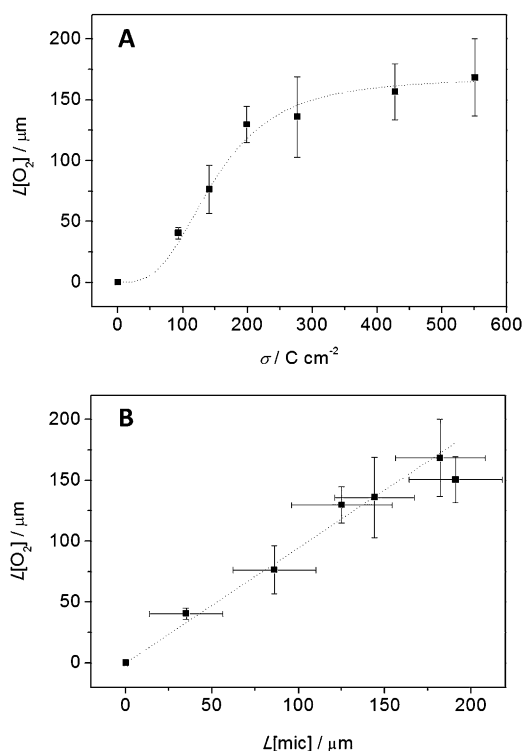


**Figure 2.** A) Increase in biofilm thickness, obtained by using the electrochemical method ( $L[\text{O}_2]$ ), versus the charge density  $\sigma$  at which biofilm growth was stopped. The sigmoid fit to the experimental data points is shown to help the eyes. B)  $L[\text{O}_2]$  versus biofilm thickness obtained by using the optical method  $L[\text{mic}]$ . The linear fit has a slope of 0.95, which is very close to the expected value of 1, and has a linear correlation of 0.98. Each data point represents the average of multiple experiments on  $n$  independent biofilms ( $3 \leq n \leq 4$ ). The origin data point comes from three independent blank experiments performed on Ag electrodes without a biofilm.

as a function of  $\sigma$ .<sup>[4]</sup> After an initial phase of exponential growth, the biofilm thickness reaches a plateau at  $\sigma > 200 \text{ C cm}^{-2}$ , corresponding to approximately 150  $\mu\text{m}$ , which is the self-determined thickness achieved by these biofilms in this case.<sup>[4,15]</sup> Moreover, the obtained  $L$  values fall within those reported for mixed culture and pure *Geobacter sulfurreducens* biofilms.<sup>[4,7,16]</sup>

These findings are already indicative of the reliability of the proposed electrochemical methodology. However, to further assess its accuracy, I used an optical method to estimate the

biofilm thickness. The method consisted of 1) removing the Ag tip with the attached biofilm from the electrode holder, 2) scraping part of the biofilm with a scalpel until the underlying Ag surface becomes fully visible so as to form a step between the biofilm and the Ag surface, and 3) fixing the tip with the biofilm facing the objective of a light microscope. Then, using a motorized stage, I moved the air-exposed Ag tip on the Z axis, focusing first on the biofilm and then on the bare Ag surface. The distance between these focal points gave the biofilm thickness (Figure 2,  $L[\text{mic}]$ ). The data points of the  $L[\text{O}_2]$  versus  $L[\text{mic}]$  plot lay on a straight line, passing through the origin and having a slope of 0.95 (Figure 2B). This excellent correlation between biofilm thicknesses obtained with different methods proves the accuracy of my measurements and supports the correctness of the initial assumption on the applicability of Equation (1) for noninteracting chemical agents. In fact, when a chemical agent reacts in a biofilm, its penetration can be retarded, giving higher  $t_{90}$  values and an expected  $L[\text{O}_2] > L[\text{mic}]$ .<sup>[16]</sup> However, this is not the case, as shown by the slope of the straight line in Figure 2B, which is  $< 1$ . Noteworthy,  $m$  consecutive inactivation cycles ( $3 \leq m \leq 5$ ) performed on the same electrode sample give a percentage error below 10% (not shown). Therefore, the relatively large error bars associated with  $L[\text{O}_2]$  in Figure 2 reflect the different thicknesses of biofilms grown under similar conditions rather than the precision of the analytical method. Finally, the excellent correlation between the values measured with different methods together with the monoexponential fit of the CA trace (Figure 2B and 1, respectively) justify the initial hypothesis, assuming  $\text{O}_2$  diffusion through the biofilm as the rate-limiting process of biofilm inactivation in the studied system.

### 3. Conclusions

This work is a proof-of-concept study of a new experimental strategy to measure the thickness of flat electroactive microbial biofilms attached to electrodes. In addition to the basic electrochemical setup already available in all laboratories studying these biofilms, the presented method requires only the ability to introduce a sufficient amount of  $\text{O}_2$  into the working solution bathing the biofilm. Even though the method was hereby tested for mixed culture biofilms inactivated by  $\text{O}_2$ , it is, in principle, also applicable to other biofilms and inactivating molecules, such as  $\text{CO}$ ,  $\text{CN}^-$ , and other antibiotics, but only if 1) diffusion is the rate-limiting step of biofilm inactivation, 2) the CA trace fits to a monoexponential function with a coefficient of determination  $R^2 > 0.99$ , 3)  $D_e$  is properly chosen, 4) the inactivating agent suppresses the electrocatalytic current completely, and 5) its penetration is not retarded by sorption or chemical reactions. Accuracy and flexibility are the main features of this new strategy that may, thus, become a powerful analytical tool in the hands of researchers working in the field of BESs who do not have access to expensive microscopic setups or need nondisruptive methods to monitor biofilm thickness during growth.

## Experimental Section

### Microbial Inoculum and Growth Medium

The source of the microbial inoculum was primary wastewater collected from the Waternet Wastewater Treatment Plant, Amsterdam West (The Netherlands). The bacterial growth medium (1 L) contained acetate (10 mM), sodium phosphate buffer (20 mM), NH<sub>4</sub>Cl (6 mM), KCl (4 mM), trace metals (12.5 mL), and vitamin solutions (12.5 mL) having the composition described by Kim et al.<sup>[17]</sup> All solutions were purged with N<sub>2</sub> before biofilm growth.

### Primary and Secondary Biofilm Formation

For primary biofilm formation, 5 mL of wastewater per 1 L of bacterial growth medium were inoculated in a sealed electrochemical cell incubated at 35 °C under anaerobic conditions, operating in batch mode.<sup>[18]</sup> A constant potential of +0.15 V versus SCE (Amel, Italy) was applied to the working electrode (graphite rods, Mersen, France) by using a  $\mu$ Autolab potentiostat (Metrohm, Utrecht, The Netherlands) to promote biofilm formation. Afterwards, the primary biofilm enriched in *Geobacter* species<sup>[19]</sup> scraped from the carbon electrode under anaerobic conditions was used as inoculum for the secondary biofilm formation, following a similar procedure on homemade Ag disks (purity > 99.99%, diameter = 2.5 mm) at the applied potential of -0.085 V versus SCE. These polycrystalline Ag electrodes have a removable tip, allowing for fast and leakage-free tip exchange, which could rapidly be fixed under the microscope for optical measurements (SMARTIP Electrodes, VU University). Immediately before biofilm formation, the Ag electrodes were polished as described elsewhere.<sup>[20]</sup> After biofilm formation, the Ag electrodes were quickly transferred from the cell to the spectroelectrochemical cell operating in flow mode.

### Electrochemical Setup

Electrochemical measurements on the microbial biofilm were carried out in a homemade spectroelectrochemical cell, operating in a three-electrode configuration and controlled by a PGSTAT101 potentiostat (Metrohm, Utrecht, The Netherlands). The cell was equipped with a flow system controlled by a HPLC pump K-501 (Knauer, Germany), allowing for fast exchange of the solution in contact with the biofilm.<sup>[10]</sup> Current densities are expressed with respect to the projected electrode area of the working electrode. Biofilm growth was performed in a thermostated glass vessel, using a Pt coil and a SCE as the counter and the reference electrodes, respectively. All potentials provided in the manuscript are referred to the SCE reference electrode (+0.244 V vs. SHE).

### Optical Setup

Optical measurements were performed on a Renishaw Raman setup (Wotton-under-Edge, United Kingdom) equipped with a Leica light microscope with 5 $\times$  air objective and a Renishaw MS 20 Encoded Stage 100 nm motorized stage.

### Data Fitting

The CA traces were fitted to the exponential decay using an Origin Pro software (OriginLab, Northampton, MA), applying built-in non-linear curve fitting routines.

### Acknowledgements

Jan-Hein Hooijschuur is acknowledged for assistance with optical measurements, Roald Boegschoten (VU Universiteit mechanical workshop) for invaluable technical support, Dr. Gert van der Zwan for critical reading of the manuscript, Waternet Wastewater Treatment Plant Amsterdam West for providing the wastewater, and the Netherlands Organisation for Scientific Research NWO (Veni grant 722.011.003) for funding.

**Keywords:** bioelectrochemical systems • biofilm thickness • electrochemistry • *Geobacter sulfurreducens* • oxygen

- [1] D. R. Lovley, *Curr. Opin. Biotechnol.* **2008**, *19*, 564–571.
- [2] D. R. Bond, D. R. Lovley, *Appl. Environ. Microbiol.* **2003**, *69*, 1548–1555.
- [3] G. Reguera, K. P. Nevin, J. S. Nicoll, S. F. Covalla, T. L. Woodard, D. R. Lovley, *Appl. Environ. Microbiol.* **2006**, *72*, 7345–7348.
- [4] B. Virdis, F. Harnisch, D. J. Batstone, K. Rabaey, B. C. Donose, *Energy Environ. Sci.* **2012**, *5*, 7017–7024.
- [5] A. Egner, S. W. Hell, in *Handbook of Biological Confocal Microscopy*, 3rd ed., (Ed. J. B. Pawley) Springer Science + Business Media, LLC, New York, **2006**, pp.404–413.
- [6] N. Everall, *J. Appl. Spectrosc.* **2000**, *54*, 1515–1520.
- [7] J. T. Babauta, H. D. Nguyen, T. D. Harrington, R. Renslow, H. Beyenal, *Biotechnol. Bioeng.* **2012**, *109*, 2651–2662.
- [8] D. Millo, F. Harnisch, S. A. Patil, H. K. Ly, U. Schröder, P. Hildebrandt, *Angew. Chem. Int. Ed.* **2011**, *50*, 2625–2627; *Angew. Chem.* **2011**, *123*, 2673–2675.
- [9] S. M. Strycharz, A. P. Malanoski, R. M. Snider, A. Hi, D. R. Lovley, L. M. Tender, *Energy Environ. Sci.* **2011**, *4*, 896–913.
- [10] A. Bonifacio, D. Millo, P. H. J. Keizers, R. Boegschoten, J. N. M. Comman-deur, C. Gooijer, G. van der Zwan, *J. Biol. Inorg. Chem.* **2008**, *13*, 85–96.
- [11] K. P. Nevin, P. Zhang, A. E. Franks, T. L. Woodard, D. R. Lovley, *J. Power Sources* **2011**, *196*, 7514–7518.
- [12] P. S. Stewart, *J. Bacteriol.* **2003**, *185*, 1485–1491.
- [13] P. S. Stewart, G. A. McFeters, T. C. Huang, in *Biofilms II: Process Analysis and Applications*, Wiley-Liss Inc., New York, **2000**, pp.373–405.
- [14] P. Han, D. M. Bartels, *J. Phys. Chem.* **1996**, *100*, 5597–5602.
- [15] S. M. Strycharz-Glaven, L. M. Tender, *ChemSusChem* **2012**, *5*, 1106–1118.
- [16] B. Virdis, D. Millo, B. C. Donose, D. J. Batstone, *PLOS ONE* **2014**, *9*, e89918.
- [17] J. R. Kim, B. Min, B. E. Logan, *Appl. Microbiol. Biotechnol.* **2005**, *68*, 23–30.
- [18] Y. Liu, F. Harnisch, K. Fricke, R. Sietmann, U. Schröder, *Biosens. Bioelec-tron.* **2008**, *24*, 1012–1017.
- [19] F. Harnisch, C. Koch, S. A. Patil, T. Hübschmann, S. Müller, U. Schröder, *Energy Environ. Sci.* **2011**, *4*, 1265–1267.
- [20] D. Millo, A. Ranieri, W. Koot, C. Gooijer, G. van der Zwan, *Anal. Chem.* **2006**, *78*, 5622–5625.

Received: December 12, 2014

Published online on January 12, 2015

This version is different from the EarlyView version in that a correction was made to Figure 2.